LA-UR--91-1517

DE91 013520

TITLE Ab Initio Cluster Studies of La_2CuO_4

AUTHOR(S) Richard L. Martin, T-12

SUBMITTED TO NATO Advanced Research Workshop Proceedings
Cluster Models for Surface and Bulk Phenomena
Erice, Sicily, April 19-26, 1991

DISCLAIMER

Los Alamos National Laboratory
Los Alamos, New Mexico 87545

Ab Initio Cluster Studies of La_2CuO_4

Richard L. Martin

Theoretical Division, MS B268

Los Alamos National Laboratory

Los Alamos, NM 87545

1.0 Introduction

The discovery of the first high temperature cuprate superconductor by Bednorz and and Muller[1] has spurred enormous experimental and theoretical activity attempting to determine the "unique" aspects of the electronic structure of these materials[2]. The straightforward application of local-density-functional (LDF) band theory predicts the parent compound La_2CuO_4 to be a metal, when it is in fact an anti-ferromagnetic insulator with a gap of ~2eV. Local Coulomb interactions are certainly at the heart of the anti-ferromagnetism and so one goal of electronic structure theory has been to develop simple models which capture these effects and can then be extended to the infinite system. At one extreme in the first priniciples approaches to this problem are the constrained LDF methods[3,4]. They essentially carve out a local region of space within the LDF band structure in order to generate the parameters for a tight-binding model including the appropriate Coulomb interactions. The latter are determined by monitoring the total energy of the system as a function of the charge constrained to reside within the local region. At the other extreme lie first principles cluster approaches[5,6,7] whose essential philosophy is that the parameters characterizing a small cluster should be transferrable to the solid and largely determine its properties. Although the local interactions can be treated with great sophistication in this approach, approximations must be made concerning the treatment of the background used to imbed the cluster. Most efforts utilize a point-charge background for these materials; an extremely different environment from the metallic background of the constrained LDF approaches. The "truth" presumably lies somewhere between these two extremes.

In this paper we examine the properties of small cluster models of La_2CuO_4. In Section 2, the Madelung/Pauli background potential used to imbed the primary cluster and the basis sets used to expand the cluster wavefunction

1. J.G. Bednorz and K.A. Muller, Z.Phys. B 64, 189 (1986).

2. For recent reviews see High Temperature Superconductivity, K.S. Bedell, D.Coffey, D.E. Meltzer, D.Pines, and J.R.Schrieffer, eds., Addison Wesley (1990).

3. M.S. Hybertsen, M. Schluter, and N.E. Christensen, Phys. Rev. B 39, 9028(1989).

4. A.K. McMahan, J.F. Annett, and R.M. Martin, Phys. Rev. B 42, 6268 (1990).

5. Y. Guo, J.-M. Langlois and W.A. Goddard III, Science 239, 896 (1988).

6. R.L. Martin and P.W. Saxe, Intern. J. Quantum Chem. Symp. 22, 237 (1988).

7. H. Kamimura and M. Eto, J. Phys. Soc. Japan 59, 3053 (1990).

are discussed. Section 3 presents the results of calculations on CuO_6 in which the optical absorption and the photoemission spectrum are examined. The calculation on CuO_6 and our earlier work on larger clusters suggest that a single-band Pariser-Parr-Pople (PPP) model be developed. Therefore, in Section 4 the PPP model and extensions which relax the zero-differential-overlap (ZDO) approximation upon which it is based are reviewed. Calculations on the states of Cu_2O_7 necessary to parameterize the PPP model are presented in Section 5 and compared with analogous calculations for Cu_2O_{11}. Section 6 discusses the problems associated with the direct ab initio determination of the anti-ferromagnetic exchange interaction, examines the magnitudes of the occupation-dependent hopping and direct exchange interactions which arise when the ZDO approximation is relaxed, and provides estimates of the uncertainties in the parameters due to electron correlation and polarization effects not recoverable with the present basis sets and finite clusters. A comparison of the parameters with those extracted from constrained LDF theory concludes Section 6. Finally, Section 7 summarizes the conclusions of this research.

2.0 Computational Details

The MESA[8] suite of electronic structure codes were used for all calculations.

2.1 Cluster Background

2.1.1 Madelung Contribution

The point charge field which surrounds the CuO_6 cluster is generated by replicating the basic unit pictured in Figure 1. The positions of the ions correspond to those determined for the tetragonal phase of $La_{1.85}Sr_{.15}CuO_4$[9]. Formal ionic charges of +2,-2, and +3 were assigned to Cu, O, and La, respectively. Note that the ions at the periphery of the basic cell shared by more than one cell are represented by the appropriate fractional charge so that the total charge in the basic unit is zero.

Various approximations to the Madelung potential are generated by translating the basic cell along the $\hat{x}$, $\hat{y}$, and $\hat{z}$ axes. We denote these backgrounds by the number of cells in each direction, e.g. the basic cell is 111, the collection of ions obtained when it is translated forward and backward one unit along $\hat{x}$ as 311, etc.

Table 1 presents the electrostatic potential,

$$V_i = \sum_{j \neq i} \frac{q_j}{R_{ij}} \qquad \text{(EQ 1)}$$

generated at the atomic sites in the central CuO_6 cluster as a function of increasingly complete background fields. Also included for comparison in Table 1 is the Madelung potential, the sum over the infinite lattice.

TABLE 1. Point Charge Potentials at the Nucleus(eV)[a]

	PC331	PC333	PC553	M333	Madelung
Cu	-26.91	-29.26	-29.47	-28.64	-28.62
O_{eq}	22.40	20.14	22.07	20.99	20.98
O_{ax}	23.00	20.32	21.55	20.22	20.22
La	-26.34	-28.67	-26.78	-28.03	-27.95

a. EQ 1.

A rather small number of point charges picks up the bulk of the Madelung potential and generates a field in the central region which essentially differs by a constant from the exact sum[10]. Much of the absolute error can be removed by rather small adjustments of the charges at the outer edge of the point charge field. For example, the error of 1.15eV at the central Cu in the 553 background can be eliminated by replacing the charges of q=+0.25 on the 8 Cu ions furthest removed from the origin with charges of q=+0.01. These atoms, at the corners of a cube, are sufficiently distant from the central unit so that the modification to the potential is essentially spherically symmetric. The relative errors in the central cluster are therefore unaffected. For example, with this modification, the 553 background yields the exact potential at the Cu site, by design, and errors of -0.06, +0.17, and -0.02 eV at the O_{eq}, O_{ax}, and La sites, respectively.

The point charge background utilized for the CuO_6 calculations described below was generated by a modification

8. P.W. Saxe, B.H. Lengsfield III, R.L. Martin, and M. Page.

9. R. J. Cava, A. Santoro, D.W. Johnson, Jr., and W.W. Rhodes, Phys. Rev. B, 35,6716(1987).

10. N.W. Winter and R.M. Pitzer,

of the 333 field. Six additional ions were placed at positions $(\pm R_x,0,0)$, $(0,\pm R_y,0)$, and $(0,0,\pm R_z)$. The positions and accompanying charges are chosen so as to reproduce the Madelung potential at each nucleus in the primary CuO_6 cluster. In order to preserve the D_{4h} symmetry of the tetragonal phase, the constraints $R_x=R_y$ and $q_x=q_y$ were imposed. In addition, the constraint of charge neutrality implies $q_z=-2q_x$. This leaves three parameters q_x, R_x, and R_z which can be determined so as to reproduce the Madelung potentials at the three distinct sites in the primary CuO_6 unit. This procedure yields $q_x=10.6$, $R_x=19.28$Å, and $R_z=19.66$Å. The resulting potentials are given in the column labeled M333 in Table 1, where it can be seen that the error at the La site, which was not included in the fit, is -0.1 eV.

An analogous procedure was used for Cu_2O_{11}. In this case, two of the units in Figure 1 are combined to form a doubled cell. Charges of magnitude ~ $\pm 0.5e^-$ placed ~ 6Å from the central O of Cu_2O_{11} supplement a 333 background of point charges. This closely reproduces (±0.05eV) the Madelung potential at all sites in the primary Cu_2O_{11} cluster. The Cu_2O_7 cluster is generated by replacing the four axial oxygens of Cu_2O_{11} by 2- point charges.

2.1.2 Pauli Repulsion

In the course of earlier work[11], a serious inadequacy in the bare point charge field was discovered for certain states of the cluster. In particular, the energy of the Cu 4s and 4p orbitals are placed much too low. This is because these rather diffuse orbitals feel the strong attractive potential of the Cu^{2+} and La^{3+} point charges without being required to maintain orthogonality with the ion core. For example, if the CuO_6^{11-} anion (formally $Cu^{1+}O^{2-}$) is studied, the SCF solution corresponds to a d^9s like Cu, as opposed to the d^{10} like solution one might expect. If the basis set is augmented with additional diffuse s and p functions the energy of this d^9s like state is stabilized even more. A related effect occurs in the calculation of the optical spectrum of the neutral CuO_6^{10-} cluster. Here the lowest energy charge transfer excitations are predicted to be O2p -> Cu4s,p in nature, and the magnitude of the optical gap is similarly sensitive to augmentation of the basis.

11. R.L. Martin, Physica B, *165*, 583(1990).

The neglect of the neighboring ion cores is most apparent in geometries calculated for the primary cluster. The optimum CuO bond lengths are at least 0.5Å too long; the attraction of the O to the Cu^{2+} point charge is not counterbalanced by the short range Pauli repulsion. For these reasons, effective core potentials have been used to represent the 4 Cu^{2+} and 10 La^{3+} sites which immediately adjoin the primary cluster of Figure 1. These are generated for the free ion using established techniques[12]. The complete specification of the background potential is available from the author on request.

2.2 Basis Sets

All calculations reported herein used the effective core potential and double-zeta quality basis set derived for Cu by Hay and Wadt[12]. These potentials fold only the [Ne] core into the potential; the 3s and 3p electrons are explicitly included in the valence space. This modification is quite important for calculations beyond the SCF level. The standard[13] Dunning/Hay 3s2p basis set was used for the O atom.

Benchmark calculations at the self-consistent-field(SCF), and single and double-substitution configuration-interaction(CISD) level of approximation are shown for several relevant states of Cu in Table 2. The column labeled CISD(Q) applies the Davidson correction[14] to estimate the effects of unlinked cluster contributions to the CISD energy.

Of particular interest are the ionization potential (I.P.) and electron affinity (E.A.) of $Cu^{2+}(d^9)$. The difference defines the on-site Coulomb energy, or Hubbard U; $U_d = E(d^8) + E(d^{10}) - 2E(d^9)$. The calculated U_d is in rather good agreement with the experimental result (16.7eV calculated vs. 16.3eV experiment), but this comes about, as usual, through a cancellation of errors. The ionization potential is calculated to be too low by ~0.6eV while the electron affinity is too large by ~1eV. This suggests a pair correlation energy of ~1eV which is not recovered with the present

12. P.J. Hay and W.R. Wadt, J. Chem. Phys. *82*, 270 (1985); W.R. Wadt and P.J. Hay, J. Chem. Phys. *82*,284 (1985); P.J. Hay and W.R. Wadt, J. Chem. Phys. *82*, 299 (1985).

13. T.H. Dunning and P.J. Hay in *Modern Theoretical Chemistry*, edited by H.F. Schaefer III (Plenum, New York, 1977), Vol. III.

14. E.R. Davidson and D.W. Silver, Chem. Phys. Lett. *52*, 403 (1977).

basis and level of excitation. This error is known to be primarily due to the lack of f-functions on Cu.

TABLE 2. Atomic Cu Excitation Energies(eV)

State	SCF	CISD	CISD(Q)	Expt.
$Cu^{1+}(d^{10},^1S)$	0.0[a]	0.0[b]	0.0[c]	0.0[d]
$Cu^{1+}(d^9s,^3D)$	1.41	2.90	2.97	2.81
$Cu^{2+}(d^9,^2D)$	17.60	19.30	19.38	20.3[e]
$Cu^{3+}(d^8,^3F)$	52.63	55.34	55.44	57.12
I.P.	35.0	36.0	36.1	36.7
E.A.	-17.6	-19.3	-19.4	-20.4
U_d	17.4	16.7	16.7	16.3

a. The total energy is -194.753343 a.u.
b. The total energy is -194.871430 a.u.
c. The total energy is -194.875358 a.u.
d. C.E.Moore, Atomic Energy Levels (Natl. Bur. Stand., Washington, D.C.,1952), Circular 467, Vol.2 (1959).

The O^{2-} species is not bound in the gas phase. Direct tests of the error inherent in the one-electron basis set are therefore difficult to make. The first calculation reported in Table 3 concentrates on the electron affinity of the oxygen atom in the gas phase. Note that with the 3s2p basis at the CISD level of approximation, the O^- species is not even bound relative to $O(^3P)$. As is well known, the addition of an additional more diffuse O2p function[13] is necessary to describe the increased radial extent of the optimum O^- orbitals. The row labeled 3s3p refers to a basis in which such an additional p-function (α=0.059) is added to the one-electron basis. This improvement stabilizes O^- by nearly 1eV relative to $O(^3P)$, and it is now bound by ~0.6eV at the CISD level. The experimental binding energy is 1.46eV, and so we infer that the "pair correlation error" not recovered by the present basis set is of the order of 0.9eV. Much of the remaining error is recovered with the addition of a d-type polarization function.

TABLE 3. Atomic O Excitation Energies(eV)

State	SCF	CISD	CISD(Q)	Expt.
3s2p Basis				
$O^-(p^5,^2P)$	0.0[a]	0.0[b]	0.0[c]	0.0
$O(p^4,^3P)$	-1.3	-0.4	-0.4	1.46[d]
3s3p Basis				
$O^-(p^5,^2P)$	0.0[e]	0.0[f]	0.0[g]	0.0
$O(p^4,^3P)$	-0.6	0.6	0.7	1.46[d]

a. The total energy is -74.754504 a.u.
b. The total energy is -74.813047 a.u.
c. The total energy is -74.814471 a.u.
d. H.Hotop and W.C. Lineberger, J. Phys. Chem. Ref. Data, 4, 568(1975).
e. The total energy is -74.779897 a.u.
f. The total energy is -74.853312 a.u.
g. The total energy is -74.857232 a.u.

TABLE 4. Embedded O Excitation Energies(eV)

State	SCF	CISD	CISD(Q)
3s2p Basis			
$O^{2-}(p^6,^1S)$	0.0	0.0	0.0
$O^-(p^5,^2P)$	4.6	5.4	5.4
$O(p^4,^3P)$	21.8	23.4	23.4
I.P.	17.2	18.0	18.0
E.A.	4.6	5.4	5.4
U_p	12.6	12.6	12.6
3s3p Basis			
$O^{2-}(p^6,^1S)$	0.0	0.0	0.0
$O^-(p^5,^2P)$	4.5	5.3	5.3
$O(p^4,^3P)$	21.8	23.3	23.3
I.P.	17.3	18.0	18.0
E.A.	4.5	5.3	5.3
U_p	12.8	12.7	12.7

The importance of the diffuse component in describing the gas phase anion would suggest that it might be important for the proper description of the O^{2-} species expected in the cluster. In order to test this, we performed calculations on an O atom embedded in the Madelung/Pauli potential appropriate to La_2CuO_4. Results which compare

the 3s2p basis with the 3s3p basis are shown in Table 4. The diffuse function has only a minor effect in this case. The largest difference is a preferential stabilization of the O^{2-} species by ~0.1eV in the more diffuse basis. The standard 3s2p basis is therefore expected to provide a qualitatively acceptable description of O^{2-}/O^{-} in the cluster. Finally, note that the estimate of the "atomic" U_p from these calculations is approximately constant at U_p~12.7eV for all the levels of correlation in Table 4. Once again, this should arise from a cancellation of errors, and from the unrecovered correlation energy inferred from the gas phase calculations, we expect the stability of the O^{2-} species to be underestimated relative to O^{-} by ~0.9eV.

3.0 CuO_6

3.1 CuO_6^{11-}

The electron count in this species corresponds to closed-shell $Cu^{1+}(d^{10})$ species and filled $O^{2-}(p^6)$ ligands. It therefore models the situation in which an additional electron is added to La_2CuO_4. Unlike earlier calculations[11] with just the Madelung background, an SCF calculation with the Madelung/Pauli background does indeed find a $^1A_{1g}(d^{10}p^6)$ ground state. The eigenvalues, dominant symmetry components, and other information characterizing the SCF wavefunction are reproduced in Table 5. Note that the orbital indexing in the Table corresponds to "hole" notation.

The total atomic charges from the Mulliken analysis describe the $^1A_{1g}$ state as $Cu^{+.77}\ O_{eq}^{-1.96}\ O_{ax}^{-1.97}$. These total charges can often be misleading, particularly in transition metal systems or when using extended basis sets, but nevertheless they appear reasonable in this instance. A more interesting number is the sum of the Cu3d gross orbital populations, n_d. Because the d orbitals are fairly confined in radial extent, this number is usually more in line with chemical expectations. In this case, n_d=9.78. The deviation from d^{10} is due to contributions from the Cu4s orbital. The 4s mixes somewhat with the $1a_{1g}(d_{z2})$ orbital, but mostly into the $3a_{1g}$ bonding orbital.

The highest occupied molecular orbital, $1b_{1g}$, is dominantly $Cu3d_{x2-y2}$ in character. The gross Mulliken orbital population P_d, reproduced in Table 5, describes this orbital as 61% d_{x2-y2}. The next four orbitals are also predominantly Cu3d, and their character is qualitatively in line with expectations from ligand-field theory. The remaining orbitals comprise the O2p "band" of width ~3.3eV.

TABLE 5. SCF Results for $CuO_6^{11-}(d^{10})$

Orbital	Component[a]	ε[b](a.u)	ΔE(eV)	P_d[c]	f[d]
$1b_{1g}$	d_{x2-y2}	.1983	0.0	.61	---
$1a_{1g}$	d_{z2}	.1270	1.94	.79	---
$1b_{2g}$	d_{xy}	.1269	1.94	.86	---
$1e_g$	d_{xz},d_{yz}	.1098	2.41	.87	---
$1a_{2g}$	y1-x2-y3+x4	.0023	5.33	---	---
$1e_u$	x1+x2+x3+x4				
	y1+y2+y3+y4	-.0038	5.50	---	0.27
$1a_{2u}$	z1+z2+z3+z4	-.0249	6.07	---	---
$1b_{2u}$	z1-z2+z3-z4	-.0360	6.38	---	9(-4)
$2e_g$	z1-z3				
	z2-z4	-.0466	6.66	.08	---
$2e_u$	x1-x2+x3-x4				
	y1-y2+y3-y4	-.0639	7.14	---	0.32
$2a_{1g}$	z5-z6	-.0765	7.48	.17	---
$3e_u$	x5+x6				
	y5+y6	-.0859	7.73	---	0.09
$2b_{2g}$	y1+x2-y3-x4	-.0862	7.74	.14	---
$2b_{1g}$	x1-y2-x3-y4	-.0866	7.75	.38	---
$3e_g$	x5-x6				
	y5-y6	-.0896	7.83	.04	---
$2a_{2u}$	z5+z6	-.0896	7.84	---	---
$3a_{1g}$	x1+y2-x3-y4	-.1178	8.60	-.07	---

a. The in-plane oxygens are numbered counter-clockwise with O1 along the positive x-axis and O2 along the positive y-axis. O5 lies above the plane and O6 below.
b. The eigenvalues in atomic units (1a.u.=27.21eV).
c. The percentage of Cu3d character in the orbital as determined from the gross Mulliken population.
d. The oscillator strength from the $1b_{1g}$ orbital in the length form; $f_{ij}=2/3\ \Delta E_{ij}\ |<i|r|j>|^2$.

There are two orbitals in Table 5 which will be the focus of future discussion; the two combinations of b_{1g} symmetry. They are bonding and anti-bonding with respect to the $Cu3d_{x2-y2}/O2p_\sigma$ interaction and shall be referred to as $\sigma(2b_{1g})$ and $\sigma^*(1b_{1g})$.

As a prelude to the calculations to be described in the next section, it is interesting to note that Koopmans' theorem[15] provides an overview of the nature of the states expected

in the CuO_6^{10-} "neutral" cluster. First of all, the ground state of a single hole relative to the closed-shell anion is predicted to be $^2B_{1g}(\sigma^*)$. The excited states of the hole should consist of a set of crystal-field excitons in the region 2.0-2.5 eV, followed by O2p -> Cu3d charge transfer channels beginning at roughly 5eV. "Frozen orbital" oscillator strengths for the allowed dipole transitions are given in Table 5. Most of the oscillator strength in this small cluster is concentrated in two predominantly in-plane b_{1g} -> e_u excitations.

3.2 CuO_6^{10-}

3.2.1 The Ground State: $^2B_{1g}$

As discussed above, Koopmans' theorem would imply a ground state of $^2B_{1g}$ symmetry for the neutral. Since n_d for the anion is 9.78, and P_d for the $1b_{1g}$ orbital 0.61, Koopmans' theorem suggests n_d=9.17 for the neutral ground state. The d_{x2-y2} spin density, $\rho_d=P_d(1b_{1g})$, should be ~61%.

In fact, the SCF calculation does indeed yield a $^2B_{1g}$ ground state with n_d=9.18, quite close to that expected, but this masks a significant rehybridization which takes place in the SCF calculation. As opposed to ρ_d=.61, the SCF wavefunction yields ρ_d=0.91. The unpaired spin in the σ^* orbital is nearly completely localized on the Cu. This increased d character in σ^* is countered by a decrease in σ. There is very little metal-ligand covalency in the SCF wavefunction; it is quite ionic.

This rehybridization is a reflection of the large on-site Coulomb repulsion energy among 3d electrons which typifies elements on the right side of the first transition series. A doubly occupied molecular orbital with significant d character necessarily carries a large atomic component in which the metal d-orbital is doubly occupied. Reacting to the large on-site repulsion associated with this component, the Hartree-Fock approximation reduces the metal-ligand mixing thereby generating a doubly occupied orbital predominantly on the ligand and a singly occupied orbital of mainly d character. If the SCF approximation were able to accurately reproduce the appropriate on-site Coulomb repulsion, this rehybridization would be computed correctly. However, the SCF approximation significantly overestimates U_d and it therefore takes this localization much too far. These considerations hold for more sophisticated wavefunctions such as the generalized-valence-bond(GVB)[16] and complete-active-space(CAS)[17] approximations to the extent that they do not usually include in their definition the radial correlation effects responsible for the overestimate of U_d.

Rather extensive CI calculations are required to re-establish the proper covalency. A CISD calculation which includes all single and double excitations relative to the SCF reference increases the covalency somewhat. A natural orbital analysis of the ground state has a single natural orbital with occupation number 1.003. This orbital is characterized by a gross d population P_d=0.88. The bonding b_{1g} natural orbital has P_d=0.15. This increased covalency is also reflected in the fact that the largest coefficient in the CISD wavefunction, other than the reference determinant, is a single excitation, $1b_{1g}$ -> $2b_{1g}$, with coefficient −0.05. It is unusual for a single excitation to play such an important role in the CISD wavefunction given the fact that there is no direct coupling between the SCF determinant and single excitations. If this configuration is included in the reference space and all single and double excitations relative to the two are diagonalized, the coefficient grows even larger to −0.09. The σ and σ^* natural orbitals now have P_d=0.17 and P_d=0.84, respectively. The proper covalency depends directly upon the energy difference between the basis states $|d^9p^6>$ and $|d^{10}p^5>$. This excitation energy is placed much too high when using the d^9-like ground state SCF orbitals. The reasons for this are discussed in more detail in Section 3.2.3.

3.2.2 Crystal Field Excitons

Table 6 reports crystal field excitation energies computed for CuO_6^{10-}.

15. T. Koopmans, Physica *1*,104 (1933).

16. F.W. Bobrowicz and W.A. Goddard, Methods of Electronic Structure Theory, H.F. Schaefer, ed., Plenum 1977.

17. B.O. Roos, P.R. Taylor, and P.E.M. Siegbahn, Chem. Phys. 48, 157 (1980); B.O. Roos, Intern. J. Quantum Chem. . Symp. 14, 175 (1980).

TABLE 6. Crystal Field Excitation Energies(eV)

State	SCF	CISD	CISD(Q)
$^2B_{1g}(d_{x2-y2})$	0.0[a]	0.0[b]	0.0[c]
$^2B_{2g}(d_{xy})$	1.54	1.74	1.82
$^2A_{1g}(d_{z2})$	1.64	1.82	1.89
$^2E_g(d_{xz},d_{yz})$	1.98[d]	2.20	2.28

a. E_{tot}=-966.216857 a.u.
b. E_{tot}=-966.727018 a.u.
c. E_{tot}=-966.797965 a.u.
d. Symmetry equivalence restrictions were imposed in this case.

At the SCF level of approximation, these states lie in the region ~1.5-2.0eV. It should be expected that the SCF approximation is relatively good for this class of excitations since they are all essentially d^9 in character and should therefore have very similar correlation energies. This is indeed the case. The CISD excitation energies are uniformly increased by ~0.2eV over the SCF results, and the Davidson correction increases them by another ~0.1eV.

Optical transitions to these crystal field states are all forbidden by parity and gain intensity only through vibronic interactions. There apears to be no definitive experimental assignment, so the accuracy of the calculation is difficult to assess. We note that an "excitonic" feature at ~1.8eV appears in the optical spectrum[18] of La_2CuO_4, which is in the general region expected for crystal field states according to the calculation.

3.2.3 $\sigma \rightarrow \sigma^*$ Charge Transfer

A critical parameter describing the electronic structure of these systems is the difference in Cu and O on-site energies, $\Delta=\alpha_d-\alpha_p$. This parameter, along with the hopping integral t_{pd}, can be estimated from the difference in energy between the ground state, $1^2B_{1g}(\sigma^*)$, and the excited state in which the hole is in the "bonding" b_{1g} orbital, $2^2B_{1g}(\sigma)$. To a first approximation, these may be thought of as $|d^9p^6>$ like and $|d^{10}p^5>$ like, respectively. Because of large atomic relaxation effects between d^9 and d^{10}, it is surprisingly difficult to obtain a decent estimate for this excitation energy. Consider first the frozen-orbital(FO) approximation in Table 7.

TABLE 7. $\sigma \rightarrow \sigma^*$ Charge Transfer Energies(eV)

	Orbital Basis	Energy			$n_d(P_d)$
		FO	CIS	CISD	CISD
$1^2B_{1g}(\sigma^*)$	d^9 SCF	0.0	0.0	0.0	9.24(.84)
$2^2B_{1g}(\sigma)$		15.16	9.01	10.30	9.78(.17)
$1^2B_{1g}(\sigma^*)$	d^{10} SCF	0.0	0.0	0.0	9.23(.74)
$2^2B_{1g}(\sigma)$		7.75	10.60	8.25	9.58(.27)
$1^2B_{1g}(\sigma^*)$	d^9 CISNO	0.0		0.0	9.23(.79)
$2^2B_{1g}(\sigma)$		9.28		9.07	9.68(.22)
$1^2B_{1g}(\sigma^*)$	d^{10} CISNO	0.0		0.0	9.26(.79)
$2^2B_{1g}(\sigma)$		9.47		9.02	9.71(.22)

The $\sigma \rightarrow \sigma^*$ FO excitation energy is 15.2eV when computed with the ground state SCF vectors. This is expected to be too high because orbital relaxation must decrease the splitting, and in addition one expects more correlation energy in the d^{10}-like excited state which will also act to decrease the splitting. On the other hand, when the SCF orbitals of the anion are used, the excitation energy is predicted to be 7.75eV. In this case, orbital relaxation is expected to increase the splitting, whereas correlation will again tend to decrease it. Thus, differential relaxation and correlation are expected to partially cancel one another when using the anion orbitals, whereas the two effects amplify one another in the ground state orbital basis.

It is possible to show that a great deal of the difference in these two FO estimates comes from orbital relaxation effects. The column in Table 6 labeled CIS refers to a calculation in which all single excitations with respect to the two reference configurations $|\sigma>$ and $|\sigma^*>$ are included in the CI. Note that it exhibits much less dependence on the orbital basis: the excitation energies are 9.01 vs. 10.6eV when using the $^2B_{1g}$ or $^1A_{1g}$ orbitals, respectively. This is still an unacceptably large orbital bias, however. Even when a CISD calculation with respect to these two reference configurations is performed, the excitation energy differs by ~2eV depending on which orbital set is used.

In order to generate an orbital basis which biases against neither state, we constructed average natural orbitals[19] from the CIS calculations described above. These average natural orbitals diagonalize the sum of the one-particle

18. J. Humlicek, M. Garriga, and M. Cardona, Sol. State Comm. 7, 589 (1988).

density matrices for the two roots and are designated as CISNO orbitals in Table 7. Note that now the CISD calculations using either set are are in good agreement with one another ($9.05 \pm 0.05eV$). This is also true of the orbital populations P_d and hence the covalency. We find $P_d(\sigma)$=0.79, $Pd(\sigma^*)$=0.22 in the CISD natural orbitals using either CISNO basis.

The excitation energy and Mulliken populations allow us to extract estimates of the parameters Δ and t_{pd}. The eigenvalues of Table 5 provide a crude estimate of the direct O-O hopping integral t_{pp}^{xy}. This is discussed in more detail elsewhere[20]. We find Δ~6eV, t_{pd}~1.9eV, and t_{pp}^{xy}~0.8eV. These values are all significantly larger than the recent estimates of the parameters from constrained LDF theory[3,4] Δ~3.5V, t_{pd}~1.5eV, t_{pp}^{xy}~0.65eV.

3.2.4 Optical Absorption

Figure 2 reproduces the optical absorption spectrum[21] of La_2CuO_4 taken by Etamad, et al. The spectrum shows an onset for absorption at ~1.8eV with a much stronger rise occuring at ~5eV. The gap is generally believed to be associated with the onset of O2p -> Cu3d charge transfer channels.

The parameters determined above can be used to generate a crude estimate of the optical spectrum expected in the infinite solid. In the CuO_6 cluster, the σ^* orbital is stabilized by ~2.3eV from the bare on-site energy α_d. Assuming this stabilization is roughly correct for the solid, the centroid of the O2p/Cu3d charge transfer channels should occur at ~ Δ+2.3eV with a width determined by the O2p bandwidth which is roughly $8t_{pp}^{xy}$. This approach yields the "theoretical" spectrum shown in the top of Figure 2. Note that the onset of the very strong absorption at ~5eV coincides with the current estimate for the beginning of the charge-transfer band. The positions of the crystal-field excitons agree well with the weak absorption features in the region of ~2eV. These simple considerations must be verified by studies on larger clusters , but it would appear that the large value of Δ found in this work argues against the assignment of the optical gap at ~1.8eV to the charge transfer channels. They should rather be assigned to the onset at ~5eV. On the other hand, the LDF parameters predict a charge transfer onset at ~2.6eV[22], mostly because of the smaller value of Δ found in that work. I estimate that unrecovered electron correlation and background polarization effects in CuO_6 should only decrease Δ by ~1eV. It should be noted, however, that band theory suggests vacant La4f orbitals lie in the vicinity of 5eV. Explicit inclusion of the La atoms in the cluster might renormalize the O2p->Cu3d charge transfer states to lower energy. This is a possibility which should be examined.

3.3 CuO_6^{9-}

The electronic states of CuO_6^{9-} correspond to the addition of two holes relative to the closed-shell anion. We shall refer to this state as the "cation", since it has an additional hole relative to the "neutral" $^2B_{1g}$ ground state. The cation states can be probed by photoemission and the correlated nature of the two holes have been the object of much study[23].

3.3.1 A simple CI calculation

If the independent particle approximation were correct, one would expect the ground state of the cation to be generated by the addition of a second hole to the σ^* orbital of the neutral species; i.e.,

$$\Phi_1 = \sigma^{*2}(\alpha\beta) \qquad \text{(EQ 2)}$$

In the simple model space of the b_{1g} symmetry orbitals, there are two additional ways to place the two holes:

$$\Phi_2 = \frac{\sigma\sigma^* (\alpha\beta - \beta\alpha)}{\sqrt{2}} \qquad \text{(EQ 3)}$$

and

$$\Phi_3 = \sigma^2(\alpha\beta) \qquad \text{(EQ 4)}$$

In a photoemission experiment, only Φ_1 and Φ_2 carry intensity, because Φ_3 requires the simultaneous addition and excitation of a hole from the neutral ground state, and can-

19. P.O. Lowdin, Phys. Rev. 97, 1474 (1955); E.R. Davidson, Rev. Mod. Phys. 44, 451 (1972)..

20. R L. Martin and P.J. Hay, in preparation.

21. S. Etamad, D.E. Aspnes, M.K. Kelly, R. Thompson, J. -M. Tarascon and G.W.Hull, Phys. Rev. B 39, 9028 (1988).

22. M.S. Hybertsen, E.B. Stechel, M.Schluter and D.R. Jennison, Phys. Rev. B 41, 11068 (1990).

23. G.A. Sawatzky, this proceedings.

not be reached by the one-electron dipole operator. Therefore, the independent particle model suggests one should see two peaks in the photoelectron spectrum, the first corresponding to ionization of the σ^* electron from the neutral leading to final state Φ_1, and the second corresponding to ionization from the σ orbital leading to final state Φ_2. They should be separated by the $\sigma \rightarrow \sigma^*$ excitation energy discussed in the previous section, which was estimated to be ~9eV.

Suppose these three configurations are allowed to mix via configuration interaction, with (for the present) the orbitals defined by the $^2B_{1g}$ SCF ground state vectors. The results of this calculation are shown in Table 8.

TABLE 8. 3x3 CI Results[a] for CuO_6^{9-}

Root	ΔE(eV)	C_1[b]	C_2[b]	C_3[b]	n_d[c]
1	0.0	0.66	-0.75	0.04	9.1
2	14.3	0.72	0.65	-0.23	8.4
3	19.7	0.20	0.12	0.97	9.6

a. The orbitals used in the CI expansion were the SCF orbitals for the neutral ground state.

b. The coefficients in the expansion, see Eq. 2-4.

c. The Mulliken d-population.

Note that the lowest energy root, far from being dominated by the configuration $\Phi_1(\sigma^{*2})$, exhibits a strong mixing with $\Phi_2(\sigma\sigma^*)$. In fact, most of the weight for $\Phi_1(\sigma^{*2})$ is found in the second root at an energy 14.3eV. Thus some of the photoemission intensity carried by this configuration will show up in the high-energy "satellite" region of the spectrum. Experiment[24] finds a corresponding feature at ~12eV.

This is a very small CI calculation, but the qualitative nature of the ground state survives more detailed calculations and deserves comment. Note that the total Mulliken population in the lowest root is $d^{9.1}$. The neutral SCF ground state was characterized by $d^{9.2}$, and so it appears that the ionized electron is nearly all $O2p_\sigma$ in character. Many experiments which probe the total d-population on the Cu site, such as XPS chemical shifts, X-ray absorption, etc. have verified this qualitative picture of the charge distribution in the doped state[25]. These experiments gave rise to the statements "there is no Cu^{3+}" in the doped materials, or "the holes are all on the oxygen", which can be found in much of the literature on this subject. This is supported by the present calculation in so far as the experiments probe the density change upon doping. They do not support the seemingly related picture[26] of this lowest root as a "highly correlated local singlet"[27] with one hole on the Cu and another on the O:

where in the diagram we have considered only a single oxygen neighbor for simplicity.

The local singlet construction is not the state being described by the CI wavefunction in Table 8. The lowest root is well described by the two configurations

$$\Psi_1 \cong 0.66\Phi_1(\sigma^{*2}) - 0.75\Phi_2(\sigma\sigma^*) \qquad \text{(EQ 5)}$$

Recall that the neutral SCF orbitals are quite localized, σ^* being very nearly d_{x2-y2} and σ mostly $O2p_\sigma$. Φ_1 then describes a situation in which the two holes are in the d_{x2-y2} orbital. The second configuration describes a situation in which one of the holes moves onto the oxygen. The large mixing implies a strong charge transfer relaxation which screens the two holes. The average distance between the two holes in Φ_1 is increased by mixing in a single excitation in which one of the holes moves to the adjacent oxygen. The CI is describing a rehybridization accompanying ionization. The overall symmetries are both A_g, and so this effect may be viewed as a "breathing" of the effective Cu d orbital. The "Cu^{3+}" orbital is simply larger in the ionized state in order to decrease the effective on-site Coulomb repulsion between the two holes.

More insight into the nature of this state can be obtained by examining the CI wavefunction in the natural orbital representation. The natural orbitals diagonalize the one-particle reduced density matrix, and the eigenvalues provide corresponding occupation numbers. The Slater determinant defined by occupying the natural orbitals with

24. Z. Shen, J.W. Allen, J.J. Yeh, J. -S. Kang, W. Ellis, W. Spicer, I. Lindau, M.B. Maple, Y.P. Dalichaouch, M.S. Torikachvili, and J.Z. Sun, Phys. Rev. B 36, 8414 (1987).

25. See, e.g., *Earlier and Recent Aspects of Superconductivity*, J.G. Bednorz and K.A. Muller, eds., Springer Verlag, 1990.

26. F.C. Zhang and T.M. Rice, Phys. Rev. B 37, 3759 (1988).

27. H. Eskes and G.A. Sawatzky, Phys. Rev. Lett 61, 1415 (1988).

largest occupation numbers is the determinant with maximum overlap on the CI wavefunction. The natural orbitals of the lowest root consist of a new σ^* orbital, call it Σ^*, which is a nearly 50:50 mix of d_{x2-y2} and $O2p_\sigma$. It has a hole occupation number 1.85. The bonding natural orbital, Σ, is a 50:50 mix of d_{x2-y2} and $O2p_\sigma$ with hole occupation number 0.15. In this representation then, the lowest root is closely approximated by $\Psi_1 \cong \Sigma^{*2}$. The charge density in the leading natural configuration expands to ~25% d^8, ~50%d^9p^5, and ~25% d^{10}. The average charge on Cu is d^9, but this occurs because of equal admixtures of the ionic terms $d^8$and d^{10}.

The occupation number of 0.15 for the second natural orbital signifies a slight departure from this molecular orbital picture. It represents a modest tendency for the two holes to form the "local singlet". The continuous evolution from the MO wavefunction to the valence bond (VB) singlet can be described by the two configuration wavefunction:

$$\Psi_1 = (1+\lambda^2)^{-1/2}(\Sigma^{*2} - \lambda\Sigma^2) \qquad \text{(EQ 6)}$$

For λ=0, the MO approximation is exact. At the other extreme, λ=1, the VB singlet is exact. For the special case here of a 50:50 mixture, the total Cu d-population remains d^9 for all values of λ and cannot be used to distinguish the MO from the VB wavefunction (consider the H_2 molecule at r_e and r=∞). From the occupation numbers, one deduces λ=0.28. Thus there is a tendency toward the VB structure, but this state is still fairly well described in the MO limit. Before leaving this qualitative point, we note that it is not just our cluster calculations which find this result. All the more recent three-band parameter sets extracted from local density functional theory[3,4] and/or experiment[28] yield a wavefunction similar to that found here, although it is still often incorrectly envisioned as the local singlet pictured above.

3.3.2 Photoemission: an Internal CI calculation

In order to introduce all the pertinent photoionization channels, an internal CI calculation was performed. This CI involves distributing two holes in all possible ways among the valence molecular orbitals. The molecular orbitals are again defined by the $^2B_{1g}$ ground state SCF calculation. Because of the small mixing in the SCF wavefunction, we can distinguish 5 molecular orbitals which are predominantly Cu3d in character from the 18 molecular orbitals which are predominantly O2p in character. This allows the CI space to be described approximately by "d^8", "d^9p^5", and "d^{10}" configurations.

The results are presented in Figure 3. Each discrete CI eigenstate was broadened by a Gaussian of width 0.4eV, the experimental resolution quoted by Shen, et. al.[24], and the Cu3d and O2p components assigned a relative intensity ratio of 1.0. The d^9p^5 projection forms a band of states in the region from 0-6eV. The d^8 character is distributed throughout the spectrum, although most of it falls in the region 11-14eV. Qualitatively, the spectrum appears to be in good agreement with the experimental results also sketched in Figure 3. The peaks labeled A,B, and D as well as the region in the immediate vicinity of the Fermi edge have been shown to resonate with the Cu3p -> 3d excitation and therefore to contain significant d character. These features are all reproduced by this simple calculation.

We shall not discuss this spectrum in detail, since the analogous calculation with the older background potential is presented elsewhere. The major differences are that the present calculation puts somewhat more d character in the lowest root ($d^{9.1}$ vs. $d^{8.8}$ previously) and shifts the satellite features to higher binding energy by ~2eV.

3.3.3 Candidates for the ground state

The energies of the few lowest states of the internal CI are presented in Table 9.

The first few states correspond to those which would be expected in a simple ligand field model; i.e. after the ^1A_g ground state, the singlet and triplet couplings of the additional hole in the d_{z2} orbital are next, followed by the $d_{xz,yz}$ degenerate pair. Although we have labeled the states as if they were d^8 in character, these states also correspond largely to a density loss in the appropriate O2p orbitals. The state 2.36eV above the ground state is the $^3B_{2g}$ hole state proposed by Guo, et. al.[5] to be the ground state.

28. H. Eskes, G.A. Sawatzky, and L.F. Feiner, Physica C 160, 424 (1989).

TABLE 9. Internal CI Eigenstates for Two-holes

State	ΔE(eV)
$^1A_{1g}(d^2_{x2-y2})$	0.0
$^3B_{1g}(d_{z2}, d_{x2-y2})$	1.15
$^1B_{1g}(d_{z2}, d_{x2-y2})$	1.78
$^3E_g(d_{xz,yz}, d_{x2-y2})$	2.05
$^3A_{2g}(d_{xy}, d_{x2-y2})$	2.07
$^1A_{2g}(d_{xy}, d_{x2-y2})$	2.33
$^3B_{2g}(p_\pi, d_{x2-y2})$	2.36
$^1B_{2g}(p_\pi, d_{x2-y2})$	2.40
$^1E_g(d_{xz,yz}, d_{x2-y2})$	2.46
.	
.	
.	
$^3A_{1g}(p_\sigma, d_{x2-y2})$	3.68

More detailed calculations on three candidates for the ground state were carried out. Separate SCF calculations were performed for the $^1A_g(d_{x2-y2})$, the $^3B_{1g}(d_{z2})$, and the $^3B_{2g}$ (p_π) hole states and followed by CISD calculations. The results are shown in Table 10.

TABLE 10. CISD Energies for Two-holes(eV)

State	SCF	CISD	CISDQ
$^1A_{1g}(d^2_{x2-y2})$	0.0[a]	0.0[b]	0.0[c]
$^3B_{1g}(d_{z2}, d_{x2-y2})$	0.4	0.9	1.07
$^3B_{2g}(p_\pi, d_{x2-y2})$	0.9	1.75	2.09

a. E_{tot}=-966.042143 a.u.
b. E_{tot}=-966.604844 a.u.
c. E_{tot}=-966.697072 a.u.

The order of the states predicted by the internal CI is followed at all levels of approximation. The $^3B_{1g}$ state lies only 0.4eV higher than the ^1A_g in the SCF approximation. Correlation increases this to ~1eV. The corresponding crystal field excitation energy in the neutral species was ~1.9eV. Kamimura, et. al.[7] have argued on the basis of their cluster calculations that the nature of the doped hole changes from x^2-y^2 symmetry to z^2 symmetry at the doping concentrations corresponding to the maximum in T_c. This conclusion is based on a computed crossing of the d_{z2} and d_{x2-y2} hole states as a function of bond distance. The present calculations were also performed at bond distances appropriate to the maximum in T_c (~15% doping) and yet the d_{z2} hole state is still ~1eV higher. The basis sets and correlation treatments in the present work are significantly more complete than the minimum basis sets and CI's examined by Kamimura, et. al. Nevertheless, the excitation energy is small and the trend with bond distance is as they describe it; their point is well taken.

The $^3B_{2g}(p_\pi)$ state is found to lie ~1eV higher than the ground state at the SCF level of approximation, and correlation increases this difference to ~2eV. The major difference between the present work and that of Guo, *et al.*[5] lies in the more extensive correlation treatment utilized here. The p_π hole state does becomes more competitive when larger clusters are examined[29] and the full O2p band width is included. Nevertheless, we have always found the p_σ hole states to be lower in energy than the p_π[30]. This conclusion is supported by NMR experiments which definitively show the carriers in La_2CuO_4 to be of σ symmetry[2].

One final calculation was performed for CuO_6^{9-}. A CISD expansion was carried out with respect to the three configurations σ^{*2}, $\sigma\sigma^*$, and σ^2 with the orbitals defined by the SCF calculation on the ^1A_g ground state of the cation. This should relax and correlate d^{10} like configurations better than the previous expansions. The d^{10} character of the CI ground state is increased slightly from n_d~9.1 to n_d~9.2. The leading natural orbital is ~54% Cu3d, a slight increase over the 50% mixing observed in the simpler CI expansions.

The results of this section allow us to approximate a Hubbard U which characterizes the CuO_6 entity. Using the most extensive CISD(Q) results, and the relation U=E(CuO_6^{11-})+E(CuO_6^{9-})-2E(CuO_6^{10-}), one finds U~11.1eV. This value is fairly close to that inferred from calculations on Cu_2O_7 and Cu_2O_{11} discussed below.

4.0 PPP Model

If the electronic degrees of freedom associated with the O2p and Cu3d orbitals can be contracted into a single "ef-

29. R.L. Martin and P.J.Hay, in preparation.

30. See, e.g., A.R. Bishop, R.L. Martin, K.A. Muller, and Z. Tesanovic, Z. Phys.B 76, 17 (1989).

fective" d_{x2-y2} orbital on each Cu site, Cu_2O_7 and Cu_2O_{11} then become isoelectronic with H_2. The two effective 3d orbitals give rise to a bonding molecular orbital(MO)

$$\varphi_b = \frac{(\varphi_l + \varphi_r)}{\sqrt{2}} \qquad \text{(EC 7)}$$

and an anti-bonding MO

$$\varphi_a = \frac{(\varphi_l - \varphi_r)}{\sqrt{2}} \qquad \text{(EQ 8)}$$

where ϕ_l and ϕ_r correspond to the effective d orbitals on the left and right hand Cu sites.

The "neutral", undoped, system contains one electron per site and generates a triplet electronic state

$$|T1\rangle = \varphi_a\varphi_b(\alpha\alpha) \qquad \text{(EQ 9)}$$

and three singlet states

$$|S0\rangle = \frac{\varphi_b^2 + \lambda\varphi_a^2}{\sqrt{(1+\lambda^2)}}(\alpha\beta) \qquad \text{(EQ 10)}$$

$$|S1\rangle = \varphi_b\varphi_a\frac{(\alpha\beta - \beta\alpha)}{\sqrt{2}} \qquad \text{(EQ 11)}$$

$$|S2\rangle = \frac{\varphi_b^2 - \lambda\varphi_a^2}{\sqrt{(1+\lambda^2)}}(\alpha\beta) \qquad \text{(EQ 12)}$$

The cation and anion, analogous to H_2^+ and H_2^-, each give rise to two doublet states

$$|C0\rangle = \varphi_b(\alpha) \qquad \text{(EQ 13)}$$

$$|C1\rangle = \varphi_a(\alpha) \qquad \text{(EQ 14)}$$

$$|A0\rangle = \varphi_b^2\varphi_a(\alpha\beta\alpha) \qquad \text{(EQ 15)}$$

$$|A1\rangle = \varphi_b\varphi_a^2(\alpha\alpha\beta) \qquad \text{(EQ 16)}$$

The vacuum state has both orbitals empty and will be denoted $|0\rangle$, while the state with both orbitals occupied will be denoted by $|F\rangle$.

The PPP model is based on the zero-differential-overlap(ZDO) approximation, in which two-center charge distributions are ignored in the retention of two-electron integrals[31]. The familiar parameters characterizing the Hamiltonian consist of the on-site orbital energy ε, a hopping integral t, an on-site Coulomb repulsion U, and a two-center Coulomb repulsion V.

Within this model, the energies of the available states are then:

$$E_0 = 0 \qquad \text{(EQ 17)}$$

$$E_{C0} = \varepsilon + t \qquad \text{(EQ 18)}$$

$$E_{C1} = \varepsilon - t \qquad \text{(EQ 19)}$$

$$E_{T1} = 2\varepsilon + V \qquad \text{(EQ 20)}$$

$$E_{S0} \cong E_{T1} - \frac{(2t)^2}{U-V} \qquad \text{(EQ 21)}$$

$$E_{S1} = 2\varepsilon + U \qquad \text{(EQ 22)}$$

$$E_{S2} \cong E_{S1} + \frac{(2t)^2}{U-V} \qquad \text{(EQ 23)}$$

$$E_{A0} = 3\varepsilon + U + 2V + t \qquad \text{(EQ 24)}$$

$$E_{A1} = 3\varepsilon + U + 2V - t \qquad \text{(EQ 25)}$$

$$E_F = 4\varepsilon + 2U + 4V \qquad \text{(EQ 26)}$$

where the perturbation approximation appropriate for t << U-V has been used in Eqs. 21 and 23.

The logical extension of the PPP model is to relax the ZDO approximation and retain all the two-electron integrals which emerge in a minimum basis set calculation on H_2. This model will be referred to as the full valence Hamiltonian. It contains two additional terms. The first is a hybrid two-electron integral Hirsch[32] has referred to as Δt,

$$\Delta t = [ll,lr] = [rr,lr] \qquad \text{(EQ 27)}$$

31. R.G. Parr, Quantum Theory of Molecular Electronic Structure, W.J. Benjamin (1963).

32. J. Hirsch, Chem. Phys. Lett. (1990).

where

$$[ij, kl] = \int \varphi_i(1)\,\varphi_j(1)\,\frac{1}{r_{12}}\,\varphi_k(2)\,\varphi_l(2) \qquad \text{(EQ 28)}$$

The second is the two-center exchange integral

$$K = [lr,lr] \qquad \text{(EQ 29)}$$

These two terms are discussed in more detail in Section 6.

5.0 Cu_2O_7 and Cu_2O_{11}

For each of the states expected in the single band model, SCF calculations were performed to determine orbitals optimum for that state and followed by CISD calculations. As in the CuO_6 case, the molecular orbitals derived from the O1s, O2s, and Cu3s and 3p orbitals constitute the core and were frozen to excitation.

The exception to this general procedure occurs for the ground state of the neutral species. Here a two configuration GVB calculation was used to determine the optimum orbitals for the wavefunction |S0>; i.e. both the orbitals ϕ_b and ϕ_a and the mixing coefficient λ were optimized (Eq. 10). This multi-configuration SCF treatment is necessary in order to introduce the possibility of anti-ferromagnetic coupling into the zeroth-order wavefunction. The subsequent CI calculation included all single and double excitations with respect to both configurations ϕ_b^2 and ϕ_a^2.

5.1 Results

The energies of these states in Cu_2O_7 are reported in Table 11. Six of the seven relative energies in Table 11 were least-squares fit to the PPP energy expressions in order to derive the 4 PPP parameters reproduced at the bottom of Table 11. The energy E_{S0} was omitted from this fitting procedure. Note that the singlet states |S1> and |S2> are not referred to in Table 11. The energies of these states are ~U-V higher in energy than |S0>. In fact, SCF calculations on the state |S1> collapse into lower-lying singlets involving O2p->Cu3d charge transfer excitations. These intruder states will not be described by the PPP model. To the extent that they are important in describing the low energy physics as the cluster size increases, this is a deficiency of the present model.

TABLE 11. Table 1. Cu_2O_7 Energies

State	SCF	CISD	CISD(Q)
|0>	0.0[a]	0.0[b]	0.0[c]
|C0>	-6.78(-6.82)	-6.90(-7.03)	-6.88(-6.98)
|C1>	-5.28(-5.47	-5.46(-5.70)	-5.51(-5.70)
|T1>	-13.50(-13.50)	-10.95(-10.95)	-9.83(-9.83)
|S0>	-13.54	-11.02	-9.91
|A0>	-1.83(-1.79)	-1.96(-1.83)	-1.53(-1.44)
|A1>	-0.63(-0.44)	-0.75(-0.51)	-0.35(-0.16)
|F>	10.17(10.06)	10.57(10.39)	11.23(11.09)
J(meV)	37(88)	73(139)	90(169)
ε	-6.14	-6.36	-6.34
t	-0.68	-0.66	-0.64
U	19.74	14.37	12.53
V	-1.21	1.78	2.85

a. The total energy is -1550.16243 a.u.
b. The total energy is -1550.88436 a.u.
c. The total energy is -1551.02523 a.u.

Analogous calculations were performed for Cu_2O_{11} and are presented in Table 12.

TABLE 12. Cu_2O_{11} Energies(eV)

State	SCF	CISD	CISD(Q)
|0>	0.0[a]	0.0[b]	0.0[c]
|C0>	-6.90(-6.95)	-7.02(-7.15)	-7.00(-7.12)
|C1>	-5.43(-5.60)	-5.59(-5.82)	-5.61(-5.82)
|T1>	-13.91(-13.91)	-11.66(-11.66)	-10.60(-10.60)
|S0>	-13.95	-11.73	-10.68
|A0>	-2.88(-2.82)	-3.04(-2.91)	-2.69(-2.57)
|A1>	-1.66(-1.49)	-1.81(-1.58)	-1.48(-1.27)
|F>	8.33(8 22)	8.66(8.48)	9.25(9.09)
J(meV)	38(86)	69(130)	83(159)
ε	-6.27	-6.49	-6.47
t	-0.67	-0.66	-0.65
U	19.39	14.59	12.81
V	-1.36	1.31	2.33

a. The total energy is -1846.99674 a.u.
b. The total energy is -1847.94040 a.u.
c. The total energy is -1847.14654 a.u.

6.0 Discussion

6.1 PPP Model

The first point to be made about the results in Tables 11 and 12 is that the PPP model appears to give a very good fit to the directly computed energies. The parenthetical entries in each column give the predictions of the PPP model using the parameters extracted from the fit. The model reproduces the positions of all the states to within ~ ±0.2eV.

Another encouraging aspect of the calculations is that the parameters are rather weakly dependent on the size of the cluster. Comparing Table 11 with Table 12, one can see that the parameters extracted for Cu_2O_{11} at a given level of approximation are in good agreement with those determined for Cu_2O_7. The agreement would seem to lend support to the argument that the point charge background is appropriate for this material.

There is but one entry in Tables 11 and 12 which can be compared directly with experiment. That is the Heisenberg exchange constant $J=E_{S0}-E_{T1}$. Both neutron scattering and Raman measurements[2] are in agreement that J ~120-130 meV in La_2CuO_4. The thoretical value is quite sensitive to the level of correlation. At the GVB level, for both Cu_2O_7 and Cu_2O_{11}, J~38meV. This is only about 1/3 of the experimental result. At the CISD level of approximation, the ab initio value is nearly doubled to ~70meV. Applying the Davidson estimate for quadruple excitations increases the theoretical value by ~10-20 meV. Our best calculations thus give J~80-90meV, in much closer agreement with experiment, but still only ~75% of the correct value.

The direct computation of J is a formidable theoretical problem. In an absolute sense, one should perhaps be pleased that the calculation is able to reproduce the splitting to within ~30 meV. Expansion of the one-electron basis set to include f-functions on the Cu and d-functions on the O could certainly be expected to contribute 30meV to the differential correlation energy between |S0> and |T1>. In another sense, however, the error is more disturbing. Note that for large U-V,

$$J \equiv \frac{(2t)^2}{U - V} \qquad \text{(EQ 30)}$$

Now the value of the hopping integral in Tables 11 or 12 is quite insensitive to the level of correlation included in the calculation. Thus increases in the value of J imply, not surprisingly, reductions in the effective value of U-V. The surprising feature is the sensitivity. The fact that the GVB approximation gives only ~1/3 of the experimental splitting implies that U-V is overestimated by a factor of 3. Thus, meV improvements in J leverage eV modifications to the effective U-V. This behavior is apparent in the value of U-V in the Tables. Recall that these parameters are determined from ionization potentials and electron affinities of the cluster. The ground state |S0>, and hence the value of J, was not included in the fit. Note that U-V decreases from ~21eV to ~10eV in progressing from GVB to CISD(Q), mirroring the increase of ~2 in the theoretical J. The reduction in U-V is due to a decrease in the value of U and an increase in the value of V as the level of sophistication of the calculation increases. The decrease in U is expected and not surprising. The increase in V is somewhat more novel. In fact, at the SCF level, V is found to be negative. This interesting result can be traced to the artificially high energy of the cation states when symmetry restrictions are placed on the SCF wavefunction; that is,the additional hole in the cation is constrained to be symmetrically delocalized over both Cu sites so that the SCF wavefunction is a proper eigenstate of the symmetry operators of the cluster. The CI calculation introduces correlations which tend to localize the additional hole on one Cu and excite O2p electrons onto the site to screen it. These "electronic polaron" like effects are most dramatically evidenced in the fact that SCF solutions of broken symmetry[33] can be found for the cation states which lie lower in energy by ~2eV than the symmetry constrained SCF solution. In these wavefunctions, the single d-electron localizes on one Cu site and the O2p electrons polarize toward the other Cu site. This left-right correlation tends to localize holes doped into the cluster. This tendency should be enhanced further by nuclear motion in which the oxygen atoms move toward the localized hole.

6.2 Full Valence Hamiltonian

6.2.1 Occupation Dependent Hopping

Tables 11 and 12 allow one to examine those terms which arise in the full valence Hamiltonian for H_2 but are ne-

33. W. Nieuwpoort, this proceedings.

glected in the PPP model because of the zero-differential overlap (ZDO) approximation. The term Δt in the Hamiltonian destroys the particle-hole symmetry of the system. That is, the "band width" for a single electron in the valence space is

$$E_{C0} - E_{C1} = 2t_0 \qquad \text{(EQ 31)}$$

while the "band width" when a single hole is present ($3e^-$)

is

$$E_{A0} - E_{A1} = 2(t_0 - 2\Delta t) \qquad \text{(EQ 32)}$$

From Table 2, for example, the SCF splitting of the cation states is 1.47eV and significantly smaller (1.22eV) in the anion. The results in Table 2 yield (t_0, Δt)=(-0.74,+0.06), (-0.72,+0.05), and (-.70,+.05) eV at the SCF, CISD, and CISD(Q) levels. The magnitude of Δt, like t_0, is fairly insensitive to correlation.

Hirsch[32] has emphasized the possible role this term may have for promoting Cooper pairing. The sign of Δt is found to be opposite to that of t_0, which is the relationship necessary in Hirsch's model to induce pairing of holes. The magnitude of Δt found here, however, is presumably much too small to play a significant role in La_2CuO_4.

6.2.2 Direct Exchange Interaction

The other refinement to the PPP model which arises in the full valence Hamiltonian is the direct Cu-Cu exchange interaction. Its' most important influence is upon the superexchange constant J. In the limit of large U-V, the full valence Hamiltonian gives

$$J \cong -2K + \frac{[2(t_0 - \Delta t)]^2}{U - V} \qquad \text{(EQ 33)}$$

Given the magnitudes of t_0, Δt, U, and V found above, one can determine the effective K from the directly computed single-triplet splittings. This procedure gives 2K=(48,62,78) meV for Cu_2O_{11} as a function of correlation. The direct exchange is a small interaction and, like Δt, might be left out of a model. It is important to note, however, that it is of the same order of magnitude as the superexchange interaction[34] and has the opposite sign. This means that if one could calculate the "exact" values for t, U, and V in the PPP model, the predicted value of the superexchange interaction might easily be in error by a factor of 2. One should therefore not expect to reproduce both the optical gap and the superexchange energy in a PPP or Hubbard model. This will be true even when the optical gap corresponds to a traditional Mott insulator.

6.3 Error Estimates and Semi-empirical Parameters

Because it appears that the PPP model provides a good reproduction of the results, it is interesting to extract a semi-empirical value for the quantity U-V from the parameters determined thus far and the experimental J. Using the values for t_0, Δt, and K determined above in the CISD(Q) approximation, and an experimental value J~125meV, one finds U-V~8.2eV. This is approximately 2eV less than the best first principles estimate in Table 12.

There are several reasons to expect that the present calculations should overestimate U-V. The first concerns the rather limited double-zeta basis set utilized in this work. The addition of an electron to the neutral cluster yields a state with significant $Cu^{1+}(d^{10})$ character. From the atomic calculations, we know that the differential correlation energy between d^9 and d^{10} not recovered by the present bais set will preferentially stabilize the d^{10} state by ~1.0eV. Thus, the electron affinity of the neutral Cu_2O_{11} cluster is expected to decrease with improvements in the basis set by some amount $\Delta E_{corr,Cu}$. On the other hand, the cation states involve primarily a loss of density from the O2p orbitals, and so the ionization potential of the neutral is expected to increase by some pair correlation energy error $\Delta E_{corr,O}$ when the full correlation energy is recovered. $\Delta E_{corr,O}$ was estimated to be ~0.9eV earlier. From the PPP energy expressions, one can see that these improvements should transform $\varepsilon \rightarrow \varepsilon - \Delta E_{corr,O}$, and $U \rightarrow U - \Delta E_{corr,Cu}$. The intersite repulsion V is unaffected in this analysis. Therefore, basis set improvements may act to reduce the effective U by ~1eV.

Another consideration is the limited cluster size and the consequent underestimation of the long range screening contributions associated with the environment. Shell model calculations[35] suggest that the electronic polarization

34. This is the effective K necessary to fit the results of the calculations. The actual two-electron integral is ~5meV.

35. M.S. Islam, M.Leslie, S.M. Tomlinson and C.R.A. Catlow, J. Phys. C 21, L109 (1988).

energy associated with either the annihilation or creation of an electron in Cu^{2+} is of the order of 3eV. The screening associated with the creation of a hole on O^{2-} is similar, ~2eV. If we denote the portion of this energy not recovered in the present cluster by ΔE_{pol}, then analysis of the PPP energy expressions shows that inclusion of this contribution does not affect the near-neighbor interaction V, but modifies the on-site terms: $\varepsilon \rightarrow \varepsilon + \Delta E_{pol}$, and $U \rightarrow U - 2\Delta E_{pol}$. If the entire overestimate of 2eV in the directly determined U-V were associated with this effect, it would imply an unrecovered polarization energy of ~1eV which seems to be a reasonable number. More probably, basis set limitations are responsible for about half of the error, with the polarization energy accounting for the other half. In summary, an overestimate of U by about 2eV seems compatible with the known deficiencies of the present calculation.

6.4 Comparisons with previous work

The considerations above lead to the semi-empirical parameters suggested in Table 13. Estimates of the uncertainties based on the discussion of the preceeding section are ~10% in t and V, and perhaps ~20% for U. The effective single-band parameters which emerge from the LDF calculations of Hybertsen, et.al.(HSC) are also presented in Table 13 for comparison[36].

TABLE 13. Suggested PPP Parameters(eV)

	This work	HSC
ε	-5.5	-1.45
t	-0.65	-0.4
U	11	4.1
V	2.5	0.1
$\frac{t}{U-V}$	13	10

a. Hybertsen, et. al.

The value of t determined in the present work is ~50% larger than HSC and the value of U is more than twice as large. These discrepancies are outside the error estimates which I believe apply to the cluster calculation. It is interesting to note that the two approaches are in better agreement regarding the reduced parameter ($\frac{t}{U-V}$) This characterizes the strength of correlations in Hubbard models (where $U_{Hubbard}$=U-V). This quantity is ~13 in the present work and ~10 with the LDF based parameter set. Both calculations agree that the present materials fall in the intermediate to strong coupling regime.

The most interesting difference in Table 3, however, is that the present calculations find a significant contribution from the near-neighbor repulsion V. The present value, V~2.5eV, is about 2/3 of the 3.8eV expected from classical electrostatics. By contrast, the LDF based theories suggest V is completely screened away. The origin of these differences is unclear, but we note that the semi-empirical parameters which have evolved in quantum chemistry over the years generally use a value for V which is some sizeable fraction of the classical value. From this perspective then, a value of 2.5eV is quite reasonable, and the absence of a significant V in these materials would be a surprising result requiring explanation.

7.0 Conclusions

The low-lying electronic states of the Cu_2O_7 and Cu_2O_{11} clusters computed with ab initio SCF/CI techniques are well described by a single-band PPP model. Extensions of this model to include terms ignored in the ZDO approximation are found to be small. The interesting occupation dependent hopping term Δt studied by Hirsch, et. al. is found to be ~10% of the direct hopping matrix element, and apparently too small to be significant in the present materials. The effective direct Cu-Cu exchange term is of the same order of magnitude as the superexchange term, but of opposite sign. This implies that one should not expect a single value of U-V to reproduce both the optical gap and the anti-ferromagnetic exchange interaction J.

The direct ab initio computation of J is in only fair agreement with experiment (80-90 meV computed vs 120-130 meV measured). It is suggested that this is due to an overestimate of the Hubbard U by ~2eV in the ab initio calculation; of this, approximately 1eV is believed to be recoverable by improvements in the one-electron basis set, with another 1eV arising from long range screening effects not recoverable in a cluster of this size.

The present work is in basic agreement with the LDF based schemes in that the parameter $\frac{t}{U-V}$ which characterizes the strength of the correlations in a Hubbard model is in the intermediate to strong coupling regime. The two

36. E.B. Stechel, private communication.

approaches differ importantly, however, in that the present work finds V~U/5. The cluster results thus indicate that charge fluctuations may play a larger role in these materials than generally believed.

One of the more interesting results of this research is that we find that when an additional hole is doped into the half-filled band the dominant correlations among the Cu3d and O2p electrons manifest themselves in broken-symmetry SCF solutions in which the additional hole localizes on one side of the cluster. The tendency to form this "electronic polaron" is ultimately associated with the presence of the highly polarizable O mediating the effective interactions between the two Cu sites. The pertinent energy scales are the magnitude of the polarization energy gained by screening a localized hole versus the effective bandwith (the kinetic energy cost paid for localization). In molecular systems, broken symmetry hole-states are common in systems with weak through-bond interactions mediated by a polarizable connecting group. In most cases, this manifests itself in a strong on-site electron-phonon interaction and significant vibronic coupling. This strong polarization feature of the electronic structure of La_2CuO_4 is shared with $BaBiO_3$, and it is quite reasonable to expect this to be a dominant theme in that material as well.

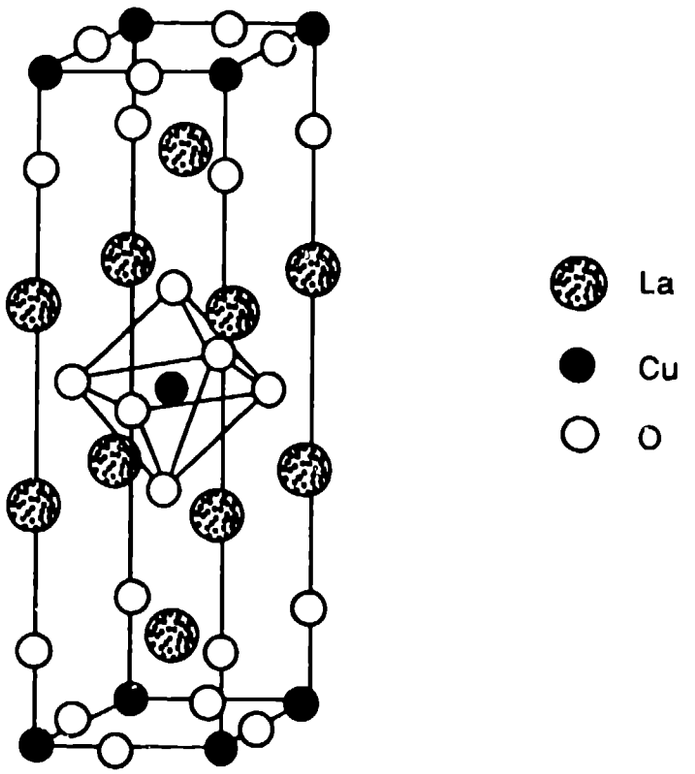
La
Cu
O

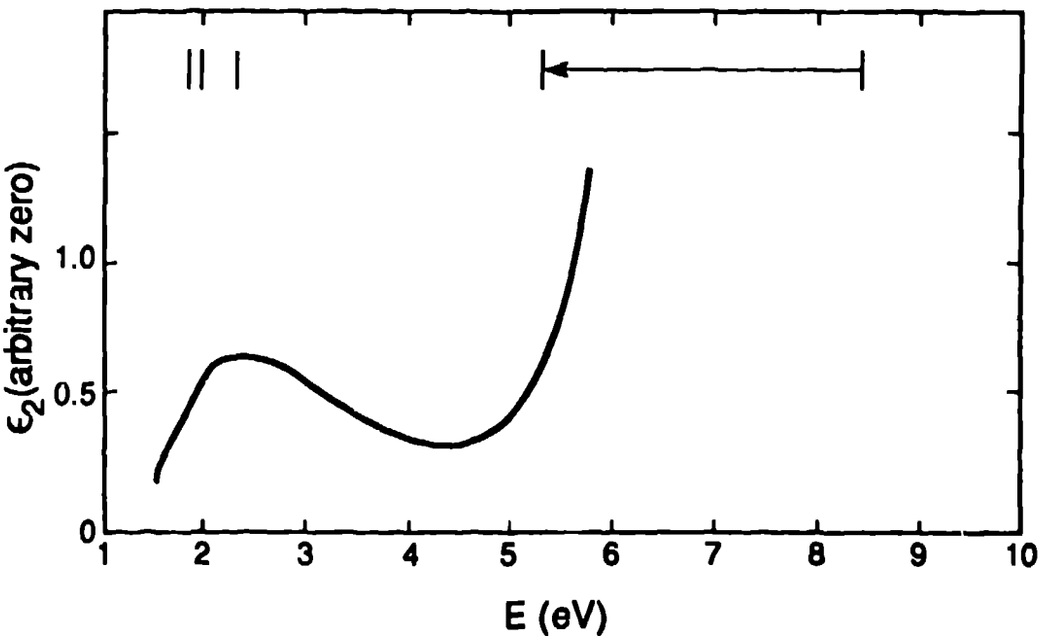
ϵ_2(arbitrary zero)
0
0.5
1.0
1
2
3
4
5
6
7
8
9
10
E (eV)

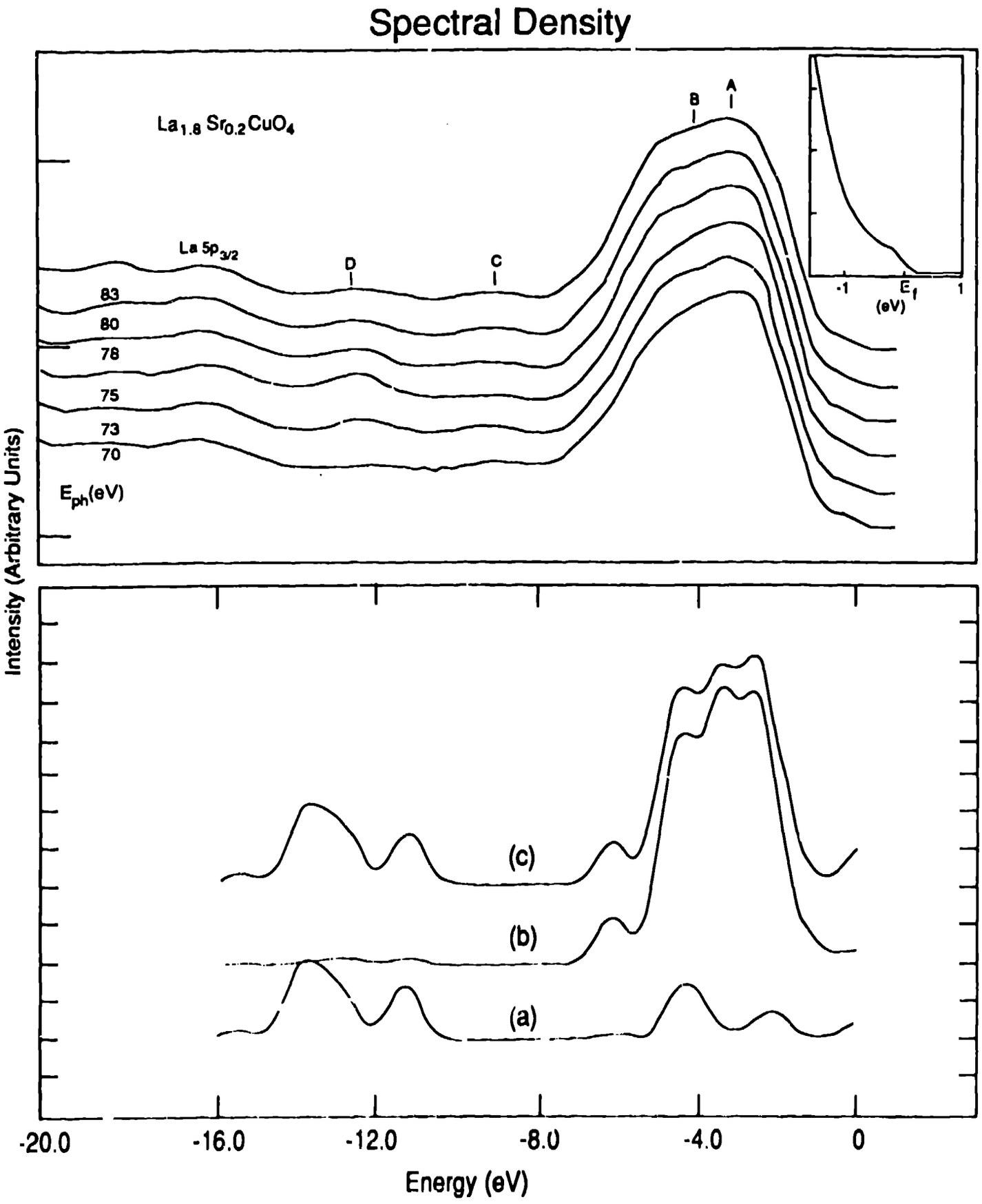
Spectral Density
La1.8 Sr0.2CuO4
La 5p3/2
A
B
C
D
83
80
78
75
73
70
Eph(eV)
-1
Ef
1
(eV)
(a)
(b)
(c)
Intensity (Arbitrary Units)
-20.0
-16.0
-12.0
-8.0
-4.0
0
Energy (eV)